Published in final edited form as:
Nat Immunol. 2014 June ; 15(6): 538–545. doi:10.1038/ni.2888.

Rad50-CARD9 interactions link cytosolic DNA sensing to IL-1β production

Susanne Roth[1], **Andrea Rottach**[2], **Amelie S. Lotz-Havla**[3], **Verena Laux**[1], **Andreas Muschaweckh**[4], **Søren W. Gersting**[3], **Ania C. Muntau**[3], **Karl-Peter Hopfner**[5], **Lei Jin**[6], **Katelynd Vanness**[7], **John H. J. Petrini**[7], **Ingo Drexler**[4,8], **Heinrich Leonhardt**[2], and **Jürgen Ruland**[1]

[1]Institut für Klinische Chemie und Pathobiochemie, Klinikum rechts der Isar, Technische Universität München, Ismaninger Str. 22, 81675 Munich, Germany

[2]Department Biology II and Center for integrated Protein Science Munich (CiPSM), Ludwig-Maximilians-Universität München, Großhaderner Str. 2-4, 82152 Martinsried, Germany

[3]Kinderklinik und Kinderpoliklinik im Dr. von Haunersches Kinderspital, Ludwig-Maximilians-Universität, Lindwurmstrasse 4, 80337 Munich, Germany

[4]Institut für Virologie, Klinikum rechts der Isar, Technische Universität München, and Helmholtz Zentrum München, German Research Centre for Environmental Health, Trogerstr. 30, 81675 Munich, Germany

[5]Gene Center and Center for integrated Protein Science Munich (CiPSM), Department of Biochemistry, Ludwig-Maximilians-Universität, Feodor-Lynen-Straße 25, 81377 Munich, Germany

[6]Center for Immunology and Microbial Disease, Albany Medical College, 47 New Scotland Avenue, Albany, NY 12208, USA

[7]Memorial Sloan-Kettering Cancer Center, 1275 York Avenue, New York, NY 10021, USA

[8]Institut für Virologie, Universitätsklinikum Düsseldorf, Heinrich Heine Universität, Universitätsstr. 1, 40225 Düsseldorf, Germany

Abstract

Double-stranded DNA (dsDNA) in the cytoplasm triggers interleukin-1β (IL-1β) production as an anti-viral host response, and deregulation of the pathways involved can promote inflammatory disease. Here we report a direct cytosolic interaction between the DNA-damage sensor Rad50 and the innate immune adapter CARD9. Dendritic cell transfection with dsDNA or infection with a DNA virus induces the formation of dsDNA-Rad50-CARD9 signaling complexes for NF-κB activation and pro-IL-1β generation. Primary cells conditionally deficient for Rad50 or lacking

Correspondence and requests for materials should be addressed to J.R. (jruland@lrz.tum.de).

AUTHOR CONTRIBUTIONS

S.R., A.R., H.L., and J.R. designed the study. S.R., A.R., A.S.L., V.L, A.M., and K.V. performed the experiments. S.R., A.R., A.S.L., S.W.G., A.C.M., K.-P. H., I.D., H.L., and J.R. analyzed the results. S.R., A.R., and A.S.L. generated the figures. J.H.J.P. and L.J. provided critical reagents, and S.R. and J.R. wrote the paper.

COMPETING INTEREST STATEMENT

The authors declare no competing financial interests.

Europe PMC Funders Author Manuscripts

CARD9 consequently exhibit defective DNA-induced IL-1β production, and *Card9*$^{-/-}$ mice have impaired inflammatory responses upon DNA virus infection *in vivo*. These results define a cytosolic DNA recognition pathway for inflammation and a physical and functional connection between a conserved DNA-damage sensor and the innate immune response to pathogens.

The appearance of double-stranded DNA (dsDNA) in the cytoplasm, which is normally a DNA-free environment, triggers potent inflammatory pathways that culminate in the production of interleukin-1β (IL-1β) and type 1 interferon (IFN). These innate immune responses alert the host to the presence of danger and are important for the regular defense against viruses and bacteria[1]. To recognize the aberrant localization of DNA, the immune system employs several cytosolic DNA receptors and associated signaling systems, which have in part overlapping and collaborative functions[1]. Central to the anti-viral IFN response is the endoplasmic reticulum-associated adaptor protein STING that is activated by the second messenger cGAMP, generated by the DNA sensor cGAS (cGAMP synthase)[2, 3]. STING subsequently engages the kinase TBK1 to mediate the phosphorylation and activation of IRF3 for IFN gene transcription[4]; in contrast, STING signaling is largely dispensable for IL-1β generation[5, 6].

The highly pro-inflammatory cytokine IL-1β provides additional security checkpoints for anti-viral immunity, particularly under circumstances in which viruses subvert the IFN system[7, 8]. IL-1β also couples innate viral recognition to anti-viral CD8$^+$ T cell responses[9, 10], and, as an endogenous pyrogen, IL-1β is responsible for fever reactions during infection. Because aberrant IL-1β production can induce severe pathological conditions, its generation needs to be tightly controlled and involves at least two distinct signals[11]. The first signal for mature IL-1β generation triggers the transcriptional upregulation of pro-IL-1β mRNA, and the second signal results in the proteolytic processing of pro-IL-1β, typically by caspase-1, within inflammasomes. The specific inflammasome for DNA-induced IL-1β processing contains the cytosolic DNA sensor AIM2[1], which engages the common inflammasome adapter protein ASC for caspase-1 activation. The transcription of pro-IL-1β is mediated by NF-κB, which is retained in an inactive form in the cytosol in unstimulated cells by binding to inhibitory IκB proteins. The activation of NF-κB by most stimuli requires the IκB kinase (IKK)-mediated phosphorylation of IκB, resulting in its ubiquitin-mediated degradation and the subsequent translocation of NF-κB dimers to the nucleus[12]. However, the exact mechanism by which the NF-κB signaling module is activated upon cytosolic DNA sensing is not well understood, but assumed to involve STING.

One innate immune cell-specific adapter protein that relays signals from pattern recognition receptors (PRRs) to inflammatory responses is CARD9[13], which possesses an N-terminal caspase recruitment domain (CARD) for the recruitment of downstream effectors as well as a coiled-coil region for protein oligomerization. Similar to most signaling adapters[14], CARD9 is multifunctionally engaged by several receptor systems depending on the specific context. PRRs that connect to CARD9 include the transmembrane Syk-coupled C-type lectin receptors (CLRs) and such cytosolic sensors as RIG-I and Nod2[15, 16, 17, 18, 19].

Europe PMC Funders Author Manuscripts

Here, we report a direct cytosolic interaction between CARD9 and the DNA-binding protein Rad50, which is also prominently involved in the eukaryotic DNA damage response (DDR)[20]. Together with Mre11 and Nbs1, Rad50 can form a DNA receptor complex (the MRN complex) that detects DNA double-strand breaks in the nucleus, subsequently triggering pathways which are required to maintain genome integrity[20]. We found that cytoplasmic dsDNA delivery by DNA transfection or virus infection results in the formation of distinct dsDNA-Rad50-CARD9 complexes, which selectively induce NF-κB signaling for IL-1β production. Our results define a DNA recognition pathway for inflammation and demonstrate a previously unrecognized direct connection between an evolutionarily conserved DNA damage sensor that translocates to the cytoplasm and an innate immune signaling system.

RESULTS

CARD9 can directly interact with the DNA binding factor Rad50

To obtain insight into the role of CARD9 in innate immunity, we performed a yeast two-hybrid screen with full-length CARD9 as the bait and searched for interaction partners in a human peripheral blood-derived cDNA library. The screening of 9.9×10^6 transformants yielded 33 bait-dependent interactors, which were analyzed further. The protein with the most frequent CARD9 yeast two-hybrid interactions was Rad50 (data not shown).

To validate a potential direct CARD9-Rad50 association in a mammalian system, we performed bioluminescence resonance energy transfer (BRET) experiments in COS7 cells. As BRET donor to acceptor energy transfer can only occur within a distance of less than 100 Å, protein-protein interactions can be analyzed within the environment of a living cell[21]. CARD9 and Rad50 fragments were subcloned in-frame with *Renilla reniformis* luciferase (Rluc) as an energy donor or yellow fluorescent protein (YFP) as an energy acceptor fluorophore[21]. In parallel, we generated Rluc and YFP fusion proteins with the CARD9 binding partner Bcl10 as a positive control[19] and also with the inflammasome DNA sensor AIM2[1]. BRET ratios above the method-specific threshold for a binary protein-protein interaction[21] were observed for CARD9-Bcl10 and CARD9-Rad50, but not for CARD9-AIM2 (Fig. 1a). Subsequent saturation experiments revealed a hyperbolic increase in BRET ratios, with increasing acceptor-to-donor ratios for CARD9 and Rad50, thereby excluding random bystander BRET. These biophysical data confirm an association between CARD9 and Rad50 in mammalian cells (Fig. 1b). To identify the region within Rad50 that interacts with CARD9, we created several Rad50 deletion mutants and performed mapping experiments using BRET. The minimal region of Rad50 that is required for CARD9 binding comprises amino acids 628–786, which is the structural domain that includes the zinc hook[20] (Fig. 1a).

Next, we investigated whether endogenous non-tagged CARD9 and Rad50 proteins could bind to each other. Immunoprecipitation experiments in THP-1 cells showed that endogenous Rad50 co-immunoprecipitated with endogenous CARD9 and *vice versa* (Fig. 1c, d). Because Rad50 has DNA binding activity, we tested the possibility that Rad50 could link dsDNA recognition to CARD9 binding. Depletion of Rad50 by repeated treatment (three times) with an antibody against Rad50 in THP-1 cell lysates resulted in the efficient

depletion of Rad50, but did not affect the amount of CARD9 in these lysates (Fig. 1e). To pull down DNA-associated proteins, we immobilized dsDNA containing a genomic sequence from vaccinia virus (VV) to agarose beads. Subsequent precipitations in the presence of Rad50 revealed that CARD9 specifically co-purified with dsDNA-beads, but not with empty control beads (Fig. 1e). CARD9 did not interact with dsDNA in the absence of Rad50 (Fig. 1e), indicating that Rad50 is required for dsDNA binding to CARD9. Together, these results indicate that Rad50 can bridge DNA binding to CARD9 engagement.

Rad50-CARD9 complexes sense dsDNA in the cytosol

We performed confocal microscopy to visualize the associations between dsDNA, Rad50 and CARD9 in primary immune cells and to investigate the cellular compartments in which these interactions occur (Fig. 2a, b). Fluorescent immunostaining of endogenous proteins revealed that, as expected, Rad50 was mainly localized to the nucleus in unstimulated bone marrow-derived dendritic cells (BMDCs)[22], whereas CARD9 exhibited a cytoplasmic distribution pattern[23] (Fig. 2a). The intracytoplasmic delivery of dsDNA resulted in the recruitment of Rad50 to dsDNA and in the formation of distinct dsDNA-Rad50 foci in the cytosol (Fig. 2a, b); these foci also contained Mre11 and Nbs1, indicating cytoplasmic dsDNA sensing by the entire MRN complex (Fig. 2c and Supplementary Fig. 1a, b). CARD9 was also recruited to the dsDNA-MRN complex aggregates and was specifically co-localized with Rad50 (Fig. 2a, b). Quantitative analysis showed Rad50-CARD9 complexes in all cells that contained cytoplasmic DNA upon transfection (Supplementary Fig. 1c, d). Cytoplasmic dsDNA-Rad50 complexes also formed in BMDCs from CARD9-deficient mice[15] (data not shown and Supplementary Fig. 1e), suggesting that the detection of cytoplasmic dsDNA by Rad50 is CARD9 independent. These findings indicate that CARD9 is secondarily recruited to DNA-sensing Rad50 complexes and suggest that the Rad50-mediated engagement of CARD9 potentially represents a signal for DNA-mediated immune responses.

CARD9 and Rad50 control DNA-induced IL-1β generation

To test the potential functions of CARD9 complexes in DNA-induced innate immunity, we transfected BMDCs with different forms of DNA and measured cytokine production. The stimulation of wild-type BMDCs with either linear synthetic poly(dA:dT), poly(dG:dC), purified genomic calf thymus DNA (CT-DNA) or circular bacterial plasmid DNA (Plasmid) resulted in a robust production of mature IL-1β and type 1 IFN (Fig. 3a, b). In contrast, BMDCs that lacked CARD9 had severe defects in IL-1β production upon transfection of all these DNA forms (Fig. 3a), though the production of IL-1β induced by Toll-like receptor (TLR) 4 stimulation with LPS or TLR9 stimulation with CpG-DNA was not affected; thus, CARD9-deficient cells are not unspecifically impairment in DNA-induced IL-1β production. Moreover, the IFN responses controlled by the cGAS-STING pathway were also unaffected by the deletion of CARD9 (Fig. 3b), whereas STING-deficient BMDCs produced substantial amounts of IL-1β but no type I IFN, consistent with previously published data (Fig. 3c, d)[5, 6]. We therefore conclude that CARD9 is specifically required for DNA-induced IL-1β responses. This conclusion was supported by additional concentration-response and kinetic studies in dsDNA-stimulated CARD9-deficient cells (Fig. 3e, f).

To study the biological relevance of these results, we transfected CARD9-deficient cells with purified microbial DNA from cowpox virus, VV or *Escherichia coli (E. coli)*. IL-1β responses to microbial genomic DNA were also specifically defective in *Card9*$^{-/-}$ BMDCs, although the IFN responses were intact (Fig. 3f, g, and data not shown), indicating a general role for CARD9 signaling during cytosolic DNA-induced IL-1β generation.

Next, we addressed if Rad50 was required for DNA-induced IL-1β generation. Rad50 is essential for cell viability during division and embryonic or hematopoietic development, and genetic deletion is embryonically lethal[20, 24, 25]. Therefore, we crossed conditional *Rad50*$^{\Delta/ind}$ mice, which carry a *Rad50* null allel together with an inducibly depleted *Rad50* allel, and *Rad50*$^{+/ind}$ mice[24], that contain one functional *Rad50* allel, to animals that ubiquitously express a tamoxifen-inducible Cre recombinase (Rosa26-CreERT2), differentiated BMDCs in culture and treated the differentiated, non-dividing BMDCs with tamoxifen to activate Cre-mediated Rad50 gene deletion *in vitro*. This protocol allowed for a substantial depletion of Rad50 from BMDCs, although the protein was not completely absent, presumably due to its long half-life (Fig. 3h). Stimulation of Rad50-depleted BMDCs with either poly(dA:dT), poly(dG:dC) or mammalian genomic DNA resulted in an up to 80% reduction in IL-1β responses compared with control cells, which still contain one functional *Rad50* allel after Cre-mediated depletion of the *Rad50*^{ind} allel. Nonetheless, parallel stimulation of Rad50-depleted cells with CARD9-independent TLR agonists or the CARD9-dependent Dectin-1 ligand curdlan induced regular IL-1β responses (Fig. 3i); thus, the Rad50-depleted cells did not exhibit a general defect in the IL-1β response. Because Rad50 activates the kinase ATM following nuclear DNA damage sensing[20], we also tested the involvement of ATM in cytosolic DNA-induced IL-1β generation. However, the production of IL-1β was not impaired by ATM deficiency[26] (Supplementary Fig. 2). Together, these genetic results establish Rad50 as an innate immune sensor for DNA and reveal that the Rad50- and CARD9-mediated DNA response operates independently of ATM to induce IL-1β.

Rad50 and CARD9 recruit Bcl10 for NF-κB activation

We next investigated the mechanisms by which the Rad50-CARD9 interaction would mediate IL-1β generation. Because CARD9 is an activator of canonical NF-κB signaling[13], we evaluated the nuclear translocation of the NF-κB subunits RelA (p65) and c-Rel in DNA-transfected *Card9*$^{-/-}$ cells. Using confocal microscopy, we observed that the activation of both NF-κB subunits was defective in *Card9*$^{-/-}$ BMDCs specifically after cytosolic DNA transfection, but not after CpG-DNA-mediated TLR9 stimulation (Fig. 4a-c). Consistent with these findings and the role of NF-κB activation in pro-IL-1β gene transcription, the induction of pro-IL-1β mRNA and the subsequent production of the pro-IL-1β polypeptide were also almost completely abrogated in DNA-transfected *Card9*$^{-/-}$ BMDCs (Fig. 4d and Supplementary Fig. 3). Moreover, cytosolic DNA-induced IL-6 and TNF transcription were also significantly reduced in CARD9-deficient cells (Supplementary Fig. 4a, b). However, and in agreement with the unaffected IFN responses observed above (see Fig. 3), the activation of IRF3 was intact in *Card9*$^{-/-}$ cells, as determined by both IRF3 phosphorylation and IRF3 nuclear translocation (Fig. 4e, f). In contrast, in STING-deficient cells, the activation of IRF3 was abolished (Fig. 4g) and the transcription of IFN-β was

entirely blocked (data not shown). When we transfected *Card9*$^{-/-}$ or STING-deficient BMDCs with cGAMP, which is a strong type 1 IFN inducer that directly activates STING[2, 3] we also observed that STING is essential for the IFN response[2, 3], while CARD9 is dispensable (Supplementary Fig. 5a, b). Next, we investigated the role of STING in DNA-induced IL-1β generation in more detail. Consistent with the almost intact IL-1β production in DNA-stimulated STING-deficient cells (Fig. 3c)[5, 6] the NF-κB dependent transcription of pro-IL-1β was not diminished in *Tmem173*$^{-/-}$ cells, and by confocal microscopy we also detected substantial translocation of both p65 and c-Rel into the nuclei of STING-deficient BMDCs (Fig. 4h, i). Together, these data indicate that CARD9 is essential for a specific pathway that mediates NF-κB activation for pro-IL-1β generation in response to cytosolic DNA sensing. Moreover, although STING contributes to optimal NF-κB responses, it is largely dispensable for the induction of pro-IL-1β gene transcription after DNA detection.

Card9 engages Bcl10 to activate NF-κB upon CLR or RIG-I ligation[15, 16, 18, 19]. Thus, we stimulated *Bcl10*$^{-/-}$ BMDCs with poly(dA:dT), poly(dG:dC), CT-DNA, or circular plasmid DNA to study the involvement of Bcl10 during the DNA-induced innate immune response. Bcl10 was essential for cytosolic dsDNA-induced NF-κB activation and IL-1β generation but not for the IL-1β production induced by TLR4 or TLR9 stimulation (Fig. 5a). Moreover, similar to CARD9, Bcl10 was essential for the upregulation of pro-IL-1β transcription but dispensable for IRF3 signaling and IFN-β synthesis (Fig. 5b, c, Supplementary Fig. 3, and data not shown). To investigate the roles of CARD9 and Bcl10 in inflammasome activation, we also assessed caspase-1 activation in CARD9- or Bcl10-deficient BMDCs. This response, which is mediated by AIM2 and ASC[1], was intact in the absence of CARD9 or Bcl10 (Fig. 5d), indicating that CARD9 and Bcl10 specifically control the signal for pro-IL-1β generation.

Based on the findings that CARD9 and Bcl10 cooperate for NF-κB activation after cytosolic DNA sensing, we next investigated whether Bcl10 was recruited to dsDNA-Rad50 complexes. Using confocal microscopy we observed that endogenous Bcl10 co-localized to dsDNA-Rad50 aggregates upon DNA transfection (Fig. 5e). Moreover, this recruitment of Bcl10 to cytosolic Rad50 was mediated via CARD9, as it was not observed in CARD9-deficient cells. Additionally, CARD9 was regularly recruited to the dsDNA-Rad50 complexes in *Bcl10*$^{-/-}$ cells (Fig. 5e), demonstrating that the initial steps of Rad50-CARD9 complex formation do not require the effector Bcl10. Thus, cytosolic DNA sensing by Rad50 and the subsequent assembly of Rad50/CARD9 complexes result in a further recruitment of Bcl10 for NF-κB activation.

Rad50-CARD9 complexes sense cytosolic viral DNA upon infection

After having established the critical functions for Rad50, CARD9 and Bcl10 in DNA-induced IL-1β production, we investigated the roles of these factors during virus infection. We used the poxvirus vaccinia virus (VV) as a model because the life cycle of poxviruses includes DNA replication in the cytoplasm[27]. Similar to the DNA transfection experiments described above, the infection of wild-type or *Card9*$^{-/-}$ BMDCs with VV resulted in the localization of Rad50 to the cytoplasmic viral DNA, which confirms that this DNA sensor is able to detect cytosolic viral infection (Fig. 6a, b and data not shown). In wild-type BMDCs,

CARD9 was co-recruited to the viral-dsDNA-Rad50 foci, resulting in the formation of viral-dsDNA-Rad50-CARD9 complexes (Fig. 6a, b) that were morphologically comparable to those observed upon synthetic dsDNA transfection (see Fig. 2). To analyze whether DNA virus sensing also induces CARD9 signaling, we measured inflammatory cytokines after VV infection in wild-type, *Card9*$^{-/-}$ and *Bcl10*$^{-/-}$ BMDCs and found that both *Card9*$^{-/-}$ and *Bcl10*$^{-/-}$ BMDCs demonstrated severely impaired IL-1β production upon VV infection *in vitro*, suggesting VV recognition activated CARD9 signaling (Fig. 6c). Similarly, the VV-induced generation of the NF-κB-controlled cytokines TNF and IL-6 was also severely impaired in *Card9*$^{-/-}$ and *Bcl10*$^{-/-}$ BMDCs (Fig. 6c). Control cell infection with the RNA virus vesicular stomatitis virus (VSV) resulted in defective IL-1β production in *Card9*$^{-/-}$ cells (Supplementary Fig. 6), which is in accord with the function of CARD9 downstream of RIG-I[17, 18, 28, 29].

To investigate the physiological significance of CARD9 in innate immune responses to DNA virus infection *in vivo*, we infected CARD9-deficient mice with VV via an intravenous route. After 6 hours, we measured the serum concentrations of IL-1β using a cytometric bead array (CBA), which revealed that the CARD9-deficient mice exhibited defective IL-1β production upon infection (Fig. 7a). Because IL-1β regulates adaptive anti-viral CD8$^+$ T cell responses[9, 10], we investigated the frequency of IFN-γ-producing virus antigen-specific CD8$^+$ T cells at 8 days after VV infection in wild-type and CARD9-deficient mice. Consistent with the diminished IL-1β production observed in CARD9-deficient mice, anti-viral CD8$^+$ T cell responses were also significantly impaired in the absence of Card9 (Fig. 7b). Thus, the Rad50/CARD9 complexes sense viral cytoplasmic DNA after cell infection and the activation of CARD9 signaling is critical for the subsequent host response *in vivo*.

DISCUSSION

Understanding cytosolic DNA recognition and downstream signaling has been a focus of intense research for several years. Multiple cytosolic DNA sensors have been described, including AIM2, cGAS, DAI, LRRFIP1, IFI16, DHX9, DDX36, DDX41 and proteins with known functions in the DDR[1, 2, 4]. Although the physiological roles of some of these receptors need to be genetically defined, experiments in gene-deficient mice have revealed the cGAS-STING signaling cascade as the key regulator of the IRF3-mediated IFN response[4, 5, 30]. Nonetheless, the disruption of STING did not affect the generation of IL-1β after DNA virus infection, although it almost completely abolished DNA-induced INF-β production[5], and we also observed that STING is largely dispensable for pro-IL-1β transcription and IL-1β generation.

Data from CARD9-and Bcl10-deficient BMDCs reveal that CARD9-Bcl10 complexes specifically control NF-κB activation and pro-IL-1β gene transcription upon cytosolic DNA sensing. The transcription of the NF-κB dependent cytokines TNF and IL-6 was also significantly reduced in DNA-stimulated CARD9-deficient cells and *Card9*$^{-/-}$ DCs show impaired TNF and IL-6 production upon DNA virus infection. Yet, because TNF and IL-6 generation is not completely defective in *Card9*$^{-/-}$ cells it is possible that STING dependent signals could contribute to the production of certain NF-κB-dependent factors beside from pro-IL-1β. It remains to be determined whether and how distinct NF-κB responses could be

differentially regulated via CARD9 and potentially STING. Because *Card9*$^{-/-}$ cells and *Bcl10*$^{-/-}$ cells exhibit regular IRF3 activation and IFN production, it is highly unlikely that CARD9-Bcl10 complexes would directly influence the cGAS-STING cascade. This hypothesis is supported by the fact that STING triggering with cGAMP induces normal IFN-β production in *Card9*$^{-/-}$ DCs. Thus, the Rad50-CARD9 signaling pathway regulates specifically NF-κB dependent innate immune responses that are required for pro-IL-1β gene transcription. The essential function of AIM2 in DNA-mediated pro-IL-1β cleavage[1] has previously been confirmed[31, 32]. Our findings and these data together provide one comprehensive mechanism for DNA-induced IL-1β generation in which CARD9 complexes can mediate pro-IL-1β generation and the AIM2 inflammasome subsequent pro-IL-1β processing. Because CARD9 is selectively expressed in myeloid cells[13] and because its deletion does not completely abolish IL-1β production, CARD9-independent mechanisms can apparently contribute to IL-1β generation, potentially as a fail-safe mechanism.

Rad50 senses DNA via its N- and C-terminal nucleotide binding domain, which associates with Mre11 and Nbs1 to form a globular DNA binding complex[20]. The Cre-loxP-mediated genetic deletion of Rad50 provides to our knowledge the first clear genetic confirmation of an essential function for Rad50 in innate immune signaling. CARD9 associates directly with Rad50. This association involves the Rad50 Zn-hook region, which is separated from the Rad50 DNA-binding domain by an approx. 50 nm long coiled-coil domain. Bcl10 is also recruited to dsDNA-Rad50 complexes via CARD9. We therefore propose a model in which, together with Mre11 and NBS1, Rad50 detects viral or transfected dsDNA in the cytosol, resulting in the recruitment of CARD9 to the Rad50 Zn-hook region and the subsequent engagement of Bcl10 for inflammatory downstream signal transduction. The identification of the mechanism through which Rad50 localizes to the cytosol requires further investigations. We speculate that these mechanisms could involve modifications on the Nbs1 protein, because this factor controls the subcellular localization of the MRN complex as demonstrated by the finding that in fibroblasts, which contain Nbs1 truncation mutants, nuclear concentrations of Mre11 and Rad50 are reduced compared to normal cells and Mre11 and Rad50 levels increase in the cytoplasm[33].

The MRN complex has previously been reported to co-localize to sites of viral replication and to elicit anti-viral defense mechanisms involving viral DNA concatemerization and, potentially, other pathways including activation of STING[34, 35, 36], although it is still unclear how Rad50 would couple to the cGAS-STING cascade. Additional DNA damage control factors, such as DNA-PK and Ku70[37, 38], were also implicated in cytosolic DNA sensing for innate immunity. Together, these studies demonstrate a more global interaction between the evolutionarily conserved DDR system and the innate immune response to pathogens. By demonstrating a direct physical and functional connection between the damage sensor Rad50 and the pro-inflammatory signaling adapter CARD9, we now provide first mechanistic insight into these interactions.

IL-1β production induced by cytosolic DNA plays a critical role in host defense[31, 32, 39]. Therefore, IL-1β provides an anti-viral selective pressure, which is highlighted by the observation that multiple viruses have evolved strategies to inhibit IL-1β production by interfering with the NF-κB signaling pathway at multiple steps[8] or by inhibiting IL-1β

signaling, for example, through the expression of soluble IL-1β receptors (vIL-1βR) which prevent the fever reaction[7, 8, 10, 40]. Several DNA viruses, such as adenovirus, have also developed strategies to inhibit Rad50 signaling, suggesting that the Rad50 pathway is a potential target for viral subversion[34, 41]. As indicated above, IL-1β is not only important for immune defense but also a significant factor in autoinflammation[11]. Endogenous DNA that is inappropriately cleared can accumulate in cytosolic compartments and drive inflammatory diseases associated with increased IFN and IL-1β levels[42, 43, 44]. These findings indicate that it will be important to investigate the contributions of Rad50-CARD9 signaling to auto-inflammatory conditions associated with cytosolic DNA responses. Ultimately, future studies on the Rad50-CARD9 pathway may lead to selective strategies for dampening DNA-induced IL-1β-driven inflammatory responses without compromising anti-viral IFN production.

METHODS

Mice

Mice deficient in CARD9[15], Bcl10[45], STING (*Tmem173*$^{-/-}$)[46], ATM[26], or ASC (*Pycard*$^{-/-}$)[47], and *Rad50*$^{\Delta/ind}$ [24] x Rosa26-CreERT2 and *Rad50*$^{+/ind}$ [24] x Rosa26-CreERT2 mice were used at 6-12 weeks of age. Animals experiments were approved by Regierung von Oberbayern.

Media and reagents

All reagents, including Poly(dG-dC) · Poly(dG-dC) acid sodium salt (poly(dG:dC), P9389), calf thymus DNA (CT-DNA, D4764), Poly(dA-dT) · Poly(dA-dT) acid sodium salt (poly(dA:dT), P0883) were purchased from Sigma, if not otherwise stated. cGAMP was obtained from Invivogen (tlrl-cga-s).The pmaxGFP Vector from Lonza was used as the circular plasmid DNA. Cell culture reagents were obtained from Invitrogen, and FCS was obtained from HyClone. Murine recombinant GM-CSF was purchased from PreproTech. CpG 1826 oligonucleotides, ultrapure LPS, and endotoxin-free DNA from *E. coli* K12 were purchased from InvivoGen, and curdlan was purchased from Wako. Poxviral genomic DNA from VV strain CVA and from cowpox virus (isolate 81/01, 5th passage in MA104 cells; originally provided by S. Essbauer, Munich, Germany) was isolated and purified from infected cell cultures, as recently described[48].

Cell culture and stimulation

COS7 cells, THP-1 cells, and BMDCs were cultured as described[18, 21]. For DNA transfection, Lipofectamine 2000 (Invitrogen) was used according to the manufacturer's protocol. Unless otherwise stated LPS (100 ng/ml), CpG (1 μM), curdlan (200 μg/ml), and ATP (5 mM) were used for stimulation. ATP was added 45 min. prior to the end of the experiment. Bone marrow from *Rad50*$^{\Delta/ind}$ x Rosa26-CreERT2 and *Rad50*$^{+/ind}$ x Rosa26-CreERT2 mice was cultured in the presence of GM-CSF for 5 days prior to the addition of 1 μM 4-hydroxy-tamoxifen (4-OHT). These dendritic cells were cultivated for another 4 to 5 days prior to analysis.

Yeast two-hybrid screen

The yeast two-hybrid screen using CARD9 as the bait was performed by Dualsystems Biotech AG. The bait construct for the yeast two-hybrid screening was generated by subcloning a cDNA encoding human CARD9 isoform 2 into the pLexA-DIR vector, and the bait was co-transformed with a human adult peripheral blood cDNA library into host strain NMY32. A total of 9.9×10^6 transformants were screened, yielding 96 transformants that grew on selective medium. Positive transformants were tested for β-galactosidase activity using a PXG β-galactosidase assay, and 77 (corresponding to 33 distinct genes) of the 96 initial positives showed β-galactosidase activity and were considered to be true positives. The library plasmids were isolated from positive clones, and the identity of positive interactors was determined by sequencing: 19 of the 77 clones contained Rad50 sequences.

BRET analysis

BRET measurements were performed in transfected COS7 cells, as described[21]. Briefly, the full-length ORFs of CARD9 (NM_052814), Bcl10 (NM_003921), and AIM2 (NM_004833) and fragments of Rad50 (NM_005732) were introduced into plasmid vectors to express N- and C-terminal fusions with Rluc or YFP. The truncated Rad50 constructs were generated by polymerase chain reaction. All eight possible combinations of the N- or C-terminally tagged Rluc (donor) or YFP (acceptor) fusions were tested for each putative interaction pair at acceptor-to-donor ratios of 3:1, unless otherwise indicated. BRET ratios were calculated based on the equation $R = (I_A/I_D) - cf$, where R is the BRET ratio, I_A is the BRET signal, I_D is the Rluc signal, and cf is a correction factor ($(I_A/I_D)_{control}$), with the co-transfection of the donor fusion-protein with YFP in the absence of the second protein of interest used as the control. The method-specific threshold for a positive protein-protein interaction was determined as a BRET ratio of 0.094 for the donor/acceptor combination that resulted in the highest BRET ratio, as previously described[21].

Co-immunoprecipitation and immunoblot analysis

THP-1 cells were lysed, and immunoprecipitations were performed as described[18]. Cell lysates or cell supernatants were subjected to standard western blotting techniques, as previously described[15]. Proteins in cell-free supernatants were extracted by methanol/chloroform precipitation. Cytosolic and nuclear extracts were prepared as described[45].

Antibodies

The primary antibodies anti-CARD9 (sc-99054), anti-Rad50 (sc-56209 and sc-74460), anti-caspase-1 p10 (sc-514), anti-Lamin B (sc-6217), anti-NF-κB p65 (sc-372), and anti-cRel (sc-71) were obtained from Santa Cruz, and anti-Bcl10 (#4237), anti-Mre11 (#4895), anti-p95/Nbs1 (#3002), anti-IRF-3 (#4302), and anti-phospho-IRF-3 (Ser396) (#4947) antibodies were obtained from Cell Signaling. Anti-CARD9 (a rabbit polyclonal antibody raised against an N-terminal peptide of CARD9) was kindly provided by Margot Thome. The secondary anti-mouse (donkey) and anti-rabbit antibodies (goat) for immunofluorescence were conjugated to Alexa Fluor 594 and Alexa Fluor 488 (Molecular Probes), respectively.

Nucleic acid affinity purification

Oligonucleotides (50 bp DNA) containing a partial sequence of the terminal repeats of VV genomic DNA were synthesized by Biomers (sense, 5′-ccatcagaaagaggtttaatatttttgtgagaccatcgaagagagaaaga-3′, and antisense, 5′-tctttctctcttcgatggtctcacaaaaatattaaacctctttctgatgg-3′), annealed to generate dsDNA, and immobilized to Strep-Tactin Superflow (IBA) resin. Nucleic acid affinity purification was performed using THP-1 cell lysates, as described[49]. For the immunodepletion of Rad50, THP-1 lysates were incubated with anti-Rad50 or isotype control antibodies immobilized on sepharose beads for up to three consecutive rounds.

Immunofluorescence staining and confocal microscopy

Immunofluorescence staining was performed using standard technology, as described[15]. Images were obtained using a TCS SP5 AOBS confocal laser-scanning microscope (Leica) with a 63×/1.4 NA Plan-Apochromat oil immersion objective. For presentation, the images were processed with Image J software http://rsb.info.nih.gov/ij/) using linear contrast enhancement on entire images.

DNA labeling by nick translation

The direct labeling of double-stranded poly(dG:dC) DNA by incorporating ATTO 647N fluorescently labeled aminoallyl-dUTP nucleotides (Jena Bioscience) was performed by nick translation, as previously described[50].

Cytokine measurement

Cytokine concentrations were determined by ELISA (BD Biosciences, eBioscience, or PBL Biomedical Laboratories) or Cytometric Bead Array (CBA, BD Biosciences) according to the manufacturer's instructions.

Real-time PCR

Total RNA was isolated and transcribed using standard methods. The specific primer pairs were as follows: IL-1β, 5′-tgtaatgaaagacggcacacc-3′ and 5′-tcttctttgggtattgcttgg-3′; TNF, 5′-tcttctcattcctgcttgtgg-3′ and 5′-ggtctgggccatagaactga-3′; IL-6 5′-gctaccaaactggatataatcagga-3′ and 5′-ccaggtagctatggtactccagaa-3′; β-actin, 5′-agacctctatgccaacacag-3′ and 5′-tcgtactcctgcttgctgat-3′. The qPCR Core kit for SYBR Green I (Eurogentec) and a LightCycler® 480 Real-Time PCR System were used as indicated by the manufacturer. The relative IL-1β mRNA expression was calculated as the ratio of the real-time PCR signal of IL-1β mRNA to that of the β-actin mRNA and normalized to a WT unstimulated control.

Viral infections

VV strain CVA and VSV Indiana (Mudd-Summer strain) were used for viral infections. VV was propagated in CV-1 cells and purified twice via ultracentrifugation through 36% sucrose cushions; the viral titers were determined by a plaque assay using CV-1 cells with crystal violet, as described[48]. VSV was propagated in baby hamster kidney (BHK-21) cells, as described[18]. *In vitro* infections were performed at the indicated multiplicities of infection (MOIs) (MOI 0.1 to MOI 10). For *in vivo* experiments, mice were injected intravenously

with 1×10^7 pfu virus in 200 μl of PBS. After 6 hours, the serum was collected to determine the IL-1β concentration. Blinding was done for injection and serum collection of mice. Splenocytes from vaccinated mice were isolated at 8 days post-infection and stimulated with the H-2K^b-restricted VV-specific peptide B8R(20-27) (TSYKFESV; 1 μg/ml) or a control peptide, OVA(257-264) (SIINFEKL; 1 μg/ml), at 37°C for 5 h in the presence of 1 μg/ml brefeldin A (Sigma-Aldrich). The cells were live/dead-stained with ethidium monoazide bromide (Invitrogen) and blocked with anti-CD16/CD32-Fc-Block (BD Biosciences); the cell surface was stained with an eFluor450-conjugated anti-CD8a antibody (eBioscience). Intracellular staining for IFNγ was performed with a FITC-conjugated anti-IFNγ antibody (BD Biosciences) using the Cytofix/Cytoperm kit (BD Biosciences) according to the manufacturer's instructions. Data were acquired using the FACS Canto II flow cytometer (BD Biosciences) and analyzed with FlowJo software (Tree Star).

Statistics

P values were determined by Student's two-tailed t test for independent samples using Microsoft Excel.

Supplementary Material

Refer to Web version on PubMed Central for supplementary material.

ACKNOWLEDGMENTS

We thank R. Ljapoci for providing technical assistance and M. Thome for providing the anti-Card9 antibody. This work was supported by the Bavarian Genome Research Network (BayGene) and an LMUexcellent grant (42595-6) to A.C.M. and by SFB grants (SFB684) from Deutsche Forschungsgemeinschaft to H.L. and J.R. K.-P.H. is supported by NIH U19AI083025, J.H.J.P. is supported by NIH GM56888, and J.R. is supported by an ERC Advanced Grant.

References

1. Paludan SR, Bowie AG. Immune sensing of DNA. Immunity. 2013; 38(5):870–880. [PubMed: 23706668]
2. Sun L, Wu J, Du F, Chen X, Chen ZJ. Cyclic GMP-AMP synthase is a cytosolic DNA sensor that activates the type I interferon pathway. Science. 2013; 339(6121):786–791. [PubMed: 23258413]
3. Wu J, Sun L, Chen X, Du F, Shi H, Chen C, et al. Cyclic GMP-AMP is an endogenous second messenger in innate immune signaling by cytosolic DNA. Science. 2013; 339(6121):826–830. [PubMed: 23258412]
4. Goubau D, Deddouche S, Reis ESC. Cytosolic sensing of viruses. Immunity. 2013; 38(5):855–869. [PubMed: 23706667]
5. Ishikawa H, Ma Z, Barber GN. STING regulates intracellular DNA-mediated, type I interferon-dependent innate immunity. Nature. 2009; 461(7265):788–792. [PubMed: 19776740]
6. Zhang Z, Yuan B, Bao M, Lu N, Kim T, Liu YJ. The helicase DDX41 senses intracellular DNA mediated by the adaptor STING in dendritic cells. Nat Immunol. 2011; 12(10):959–965. [PubMed: 21892174]
7. Epperson ML, Lee CA, Fremont DH. Subversion of cytokine networks by virally encoded decoy receptors. Immunol Rev. 2012; 250(1):199–215. [PubMed: 23046131]
8. Smith GL, Benfield CT, Maluquer de Motes C, Mazzon M, Ember SW, Ferguson BJ, et al. Vaccinia virus immune evasion: mechanisms, virulence and immunogenicity. J Gen Virol. 2013

9. Staib C, Kisling S, Erfle V, Sutter G. Inactivation of the viral interleukin 1beta receptor improves CD8+ T-cell memory responses elicited upon immunization with modified vaccinia virus Ankara. J Gen Virol. 2005; 86(Pt 7):1997–2006. [PubMed: 15958679]
10. Zimmerling S, Waibler Z, Resch T, Sutter G, Schwantes A. Interleukin-1beta receptor expressed by modified vaccinia virus Ankara interferes with interleukin-1beta activity produced in various virus-infected antigen-presenting cells. Virol J. 2013; 10:34. [PubMed: 23356675]
11. Dinarello CA, Simon A, van der Meer JW. Treating inflammation by blocking interleukin-1 in a broad spectrum of diseases. Nat Rev Drug Discov. 2012; 11(8):633–652. [PubMed: 22850787]
12. Vallabhapurapu S, Karin M. Regulation and function of NF-kappaB transcription factors in the immune system. Annu Rev Immunol. 2009; 27:693–733. [PubMed: 19302050]
13. Roth S, Ruland J. Caspase recruitment domain-containing protein 9 signaling in innate immunity and inflammation. Trends Immunol. 2013
14. Takeuchi O, Akira S. Pattern recognition receptors and inflammation. Cell. 2010; 140(6):805–820. [PubMed: 20303872]
15. Gross O, Gewies A, Finger K, Schafer M, Sparwasser T, Peschel C, et al. Card9 controls a non-TLR signalling pathway for innate anti-fungal immunity. Nature. 2006; 442(7103):651–656. [PubMed: 16862125]
16. Hara H, Ishihara C, Takeuchi A, Imanishi T, Xue L, Morris SW, et al. The adaptor protein CARD9 is essential for the activation of myeloid cells through ITAM-associated and Toll-like receptors. Nat Immunol. 2007; 8(6):619–629. [PubMed: 17486093]
17. Hsu YM, Zhang Y, You Y, Wang D, Li H, Duramad O, et al. The adaptor protein CARD9 is required for innate immune responses to intracellular pathogens. Nat Immunol. 2007; 8(2):198–205. [PubMed: 17187069]
18. Poeck H, Bscheider M, Gross O, Finger K, Roth S, Rebsamen M, et al. Recognition of RNA virus by RIG-I results in activation of CARD9 and inflammasome signaling for interleukin 1 beta production. Nat Immunol. 2010; 11(1):63–69. [PubMed: 19915568]
19. Strasser D, Neumann K, Bergmann H, Marakalala MJ, Guler R, Rojowska A, et al. Syk Kinase-Coupled C-type Lectin Receptors Engage Protein Kinase C-delta to Elicit Card9 Adaptor-Mediated Innate Immunity. Immunity. 2012
20. Stracker TH, Petrini JH. The MRE11 complex: starting from the ends. Nat Rev Mol Cell Biol. 2011; 12(2):90–103. [PubMed: 21252998]
21. Gersting SW, Lotz-Havla AS, Muntau AC. Bioluminescence resonance energy transfer: an emerging tool for the detection of protein-protein interaction in living cells. Methods Mol Biol. 2012; 815:253–263. [PubMed: 22130997]
22. Maser RS, Monsen KJ, Nelms BE, Petrini JH. hMre11 and hRad50 nuclear foci are induced during the normal cellular response to DNA double-strand breaks. Mol Cell Biol. 1997; 17(10):6087–6096. [PubMed: 9315668]
23. Goodridge HS, Shimada T, Wolf AJ, Hsu YM, Becker CA, Lin X, et al. Differential use of CARD9 by dectin-1 in macrophages and dendritic cells. J Immunol. 2009; 182(2):1146–1154. [PubMed: 19124758]
24. Adelman CA, De S, Petrini JH. Rad50 is dispensable for the maintenance and viability of postmitotic tissues. Mol Cell Biol. 2009; 29(2):483–492. [PubMed: 19001091]
25. Luo G, Yao MS, Bender CF, Mills M, Bladl AR, Bradley A, et al. Disruption of mRad50 causes embryonic stem cell lethality, abnormal embryonic development, and sensitivity to ionizing radiation. Proc Natl Acad Sci U S A. 1999; 96(13):7376–7381. [PubMed: 10377422]
26. Barlow C, Hirotsune S, Paylor R, Liyanage M, Eckhaus M, Collins F, et al. Atm-deficient mice: a paradigm of ataxia telangiectasia. Cell. 1996; 86(1):159–171. [PubMed: 8689683]
27. Roberts KL, Smith GL. Vaccinia virus morphogenesis and dissemination. Trends Microbiol. 2008; 16(10):472–479. [PubMed: 18789694]
28. Abdullah Z, Schlee M, Roth S, Mraheil MA, Barchet W, Bottcher J, et al. RIG-I detects infection with live Listeria by sensing secreted bacterial nucleic acids. EMBO J. 2012; 31(21):4153–4164. [PubMed: 23064150]

29. Kok KH, Lui PY, Ng MH, Siu KL, Au SW, Jin DY. The double-stranded RNA-binding protein PACT functions as a cellular activator of RIG-I to facilitate innate antiviral response. Cell Host Microbe. 2011; 9(4):299–309. [PubMed: 21501829]
30. Li XD, Wu J, Gao D, Wang H, Sun L, Chen ZJ. Pivotal roles of cGAS-cGAMP signaling in antiviral defense and immune adjuvant effects. Science. 2013; 341(6152):1390–1394. [PubMed: 23989956]
31. Fernandes-Alnemri T, Yu JW, Juliana C, Solorzano L, Kang S, Wu J, et al. The AIM2 inflammasome is critical for innate immunity to Francisella tularensis. Nat Immunol. 2010; 11(5): 385–393. [PubMed: 20351693]
32. Rathinam VA, Jiang Z, Waggoner SN, Sharma S, Cole LE, Waggoner L, et al. The AIM2 inflammasome is essential for host defense against cytosolic bacteria and DNA viruses. Nat Immunol. 2010; 11(5):395–402. [PubMed: 20351692]
33. Carney JP, Maser RS, Olivares H, Davis EM, Le Beau M, Yates JR 3rd, et al. The hMre11/hRad50 protein complex and Nijmegen breakage syndrome: linkage of double-strand break repair to the cellular DNA damage response. Cell. 1998; 93(3):477–486. [PubMed: 9590181]
34. Lilley CE, Schwartz RA, Weitzman MD. Using or abusing: viruses and the cellular DNA damage response. Trends Microbiol. 2007; 15(3):119–126. [PubMed: 17275307]
35. Weitzman MD, Carson CT, Schwartz RA, Lilley CE. Interactions of viruses with the cellular DNA repair machinery. DNA Repair (Amst). 2004; 3(8-9):1165–1173. [PubMed: 15279805]
36. Kondo T, Kobayashi J, Saitoh T, Maruyama K, Ishii KJ, Barber GN, et al. DNA damage sensor MRE11 recognizes cytosolic double-stranded DNA and induces type I interferon by regulating STING trafficking. Proc Natl Acad Sci U S A. 2013; 110(8):2969–2974. [PubMed: 23388631]
37. Ferguson BJ, Mansur DS, Peters NE, Ren H, Smith GL. DNA-PK is a DNA sensor for IRF-3-dependent innate immunity. Elife. 2012; 1:e00047. [PubMed: 23251783]
38. Zhang X, Brann TW, Zhou M, Yang J, Oguariri RM, Lidie KB, et al. Cutting edge: Ku70 is a novel cytosolic DNA sensor that induces type III rather than type I IFN. J Immunol. 2011; 186(8): 4541–4545. [PubMed: 21398614]
39. Saiga H, Kitada S, Shimada Y, Kamiyama N, Okuyama M, Makino M, et al. Critical role of AIM2 in Mycobacterium tuberculosis infection. Int Immunol. 2012; 24(10):637–644. [PubMed: 22695634]
40. Alcami A, Smith GL. A mechanism for the inhibition of fever by a virus. Proc Natl Acad Sci U S A. 1996; 93(20):11029–11034. [PubMed: 8855303]
41. Stracker TH, Carson CT, Weitzman MD. Adenovirus oncoproteins inactivate the Mre11-Rad50-NBS1 DNA repair complex. Nature. 2002; 418(6895):348–352. [PubMed: 12124628]
42. Boswell JM, Yui MA, Burt DW, Kelley VE. Increased tumor necrosis factor and IL-1 beta gene expression in the kidneys of mice with lupus nephritis. J Immunol. 1988; 141(9):3050–3054. [PubMed: 3262676]
43. Dombrowski Y, Peric M, Koglin S, Kammerbauer C, Goss C, Anz D, et al. Cytosolic DNA triggers inflammasome activation in keratinocytes in psoriatic lesions. Sci Transl Med. 2011; 3(82):82ra38.
44. Popovic K, Ek M, Espinosa A, Padyukov L, Harris HE, Wahren-Herlenius M, et al. Increased expression of the novel proinflammatory cytokine high mobility group box chromosomal protein 1 in skin lesions of patients with lupus erythematosus. Arthritis Rheum. 2005; 52(11):3639–3645. [PubMed: 16255056]
45. Ruland J, Duncan GS, Elia A, del Barco Barrantes I, Nguyen L, Plyte S, et al. Bcl10 is a positive regulator of antigen receptor-induced activation of NF-kappaB and neural tube closure. Cell. 2001; 104(1):33–42. [PubMed: 11163238]
46. Jin L, Hill KK, Filak H, Mogan J, Knowles H, Zhang B, et al. MPYS is required for IFN response factor 3 activation and type I IFN production in the response of cultured phagocytes to bacterial second messengers cyclic-di-AMP and cyclic-di-GMP. J Immunol. 2011; 187(5):2595–2601. [PubMed: 21813776]
47. Mariathasan S, Newton K, Monack DM, Vucic D, French DM, Lee WP, et al. Differential activation of the inflammasome by caspase-1 adaptors ASC and Ipaf. Nature. 2004; 430(6996): 213–218. [PubMed: 15190255]

48. Gasteiger G, Kastenmuller W, Ljapoci R, Sutter G, Drexler I. Cross-priming of cytotoxic T cells dictates antigen requisites for modified vaccinia virus Ankara vector vaccines. J Virol. 2007; 81(21):11925–11936. [PubMed: 17699574]

49. Burckstummer T, Baumann C, Bluml S, Dixit E, Durnberger G, Jahn H, et al. An orthogonal proteomic-genomic screen identifies AIM2 as a cytoplasmic DNA sensor for the inflammasome. Nat Immunol. 2009; 10(3):266–272. [PubMed: 19158679]

50. Cremer M, Grasser F, Lanctot C, Muller S, Neusser M, Zinner R, et al. Multicolor 3D fluorescence in situ hybridization for imaging interphase chromosomes. Methods Mol Biol. 2008; 463:205–239. [PubMed: 18951171]

Europe PMC Funders Author Manuscripts

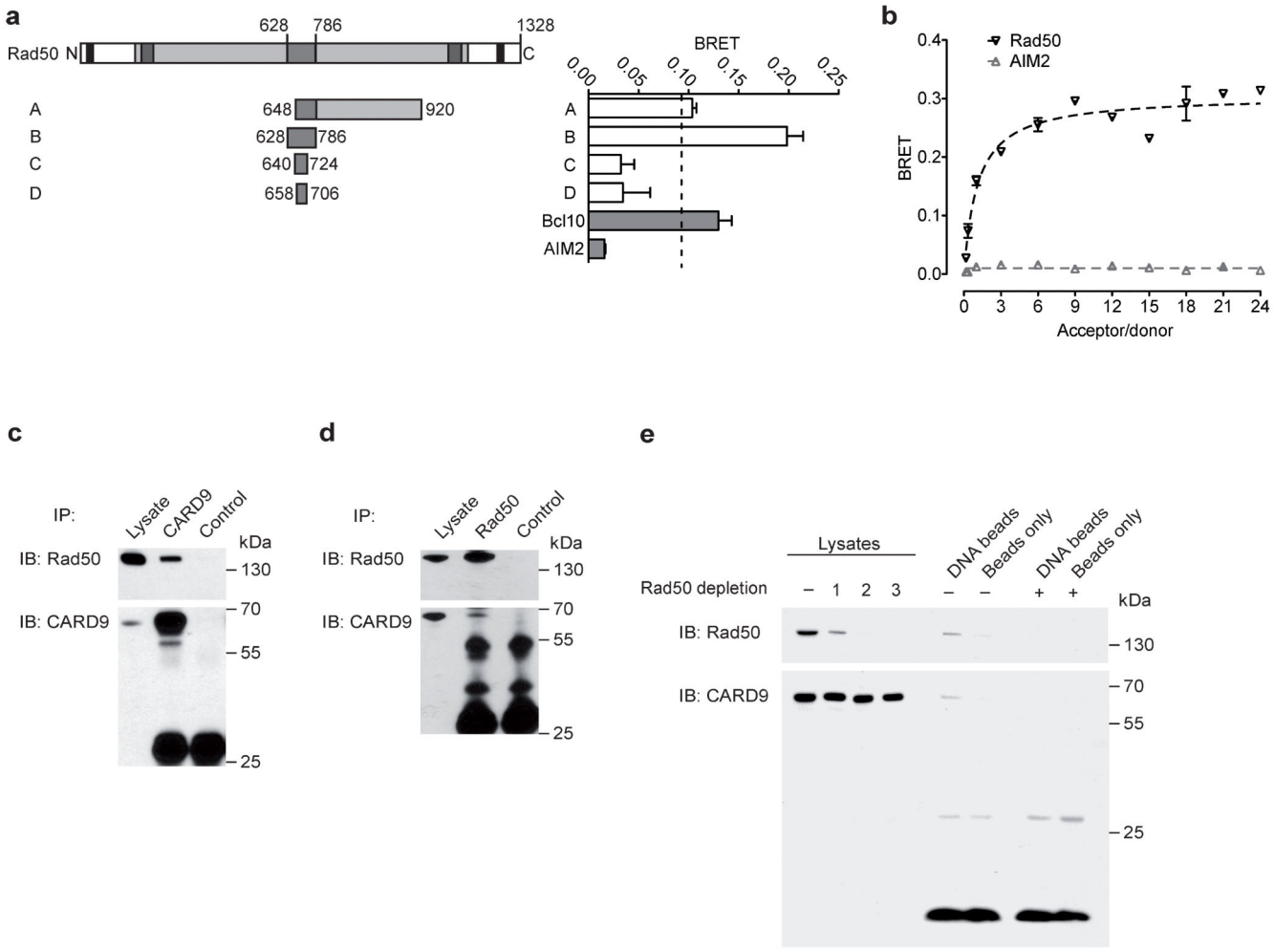

Figure 1. CARD9 interacts with Rad50

(**a**) BRET assays of binary interactions of CARD9 with Rad50 fragments, Bcl10 or AIM2 as Rluc and YFP fusion proteins in COS7 cells. The BRET ratios are given as the means + SEMs of two independent experiments. The dashed line indicates the method-specific threshold for a positive protein-protein interaction. (**b**) BRET saturation experiments using co-transfected fusions of CARD9 with Rad50 zinc hook (fragment B) orAIM2 at the indicated acceptor-to-donor ratio. The specific interaction of CARD9 with Rad50 is demonstrated by the hyperbolic behavior of BRET ratios as a function of the acceptor-to-donor ratio. (**c, d**) THP1 cell lysates were immunoprecipitated (IP) with anti-CARD9 (**c**), anti-Rad50 (**d**), or the respective isotype control antibodies. Immunoprecipitates were separated on one gel and transferred onto a single membrane, which was subsequently cut and used for immunoblot (IB) analysis with anti-Rad50 or CARD9 antibody, as indicated. (**e**) THP-1 cell lysates were left untreated (−) or were immunodepleted for Rad50 1, 2, or 3 times. Subsequently, bead-immobilized dsDNA (DNA beads) or empty streptavidin beads (Beads only) were incubated with THP-1 cell lysates that were either not treated, or immunodepleted for Rad50 three times. The beads were precipitated, and bound proteins were separated on a gel and blotted onto a single membrane. The membrane was cut and

used for western blot analysis with anti-Rad50 or CARD9 antibody, as indicated. The data are representative of at least three independent experiments (**c-e**).

Europe PMC Funders Author Manuscripts

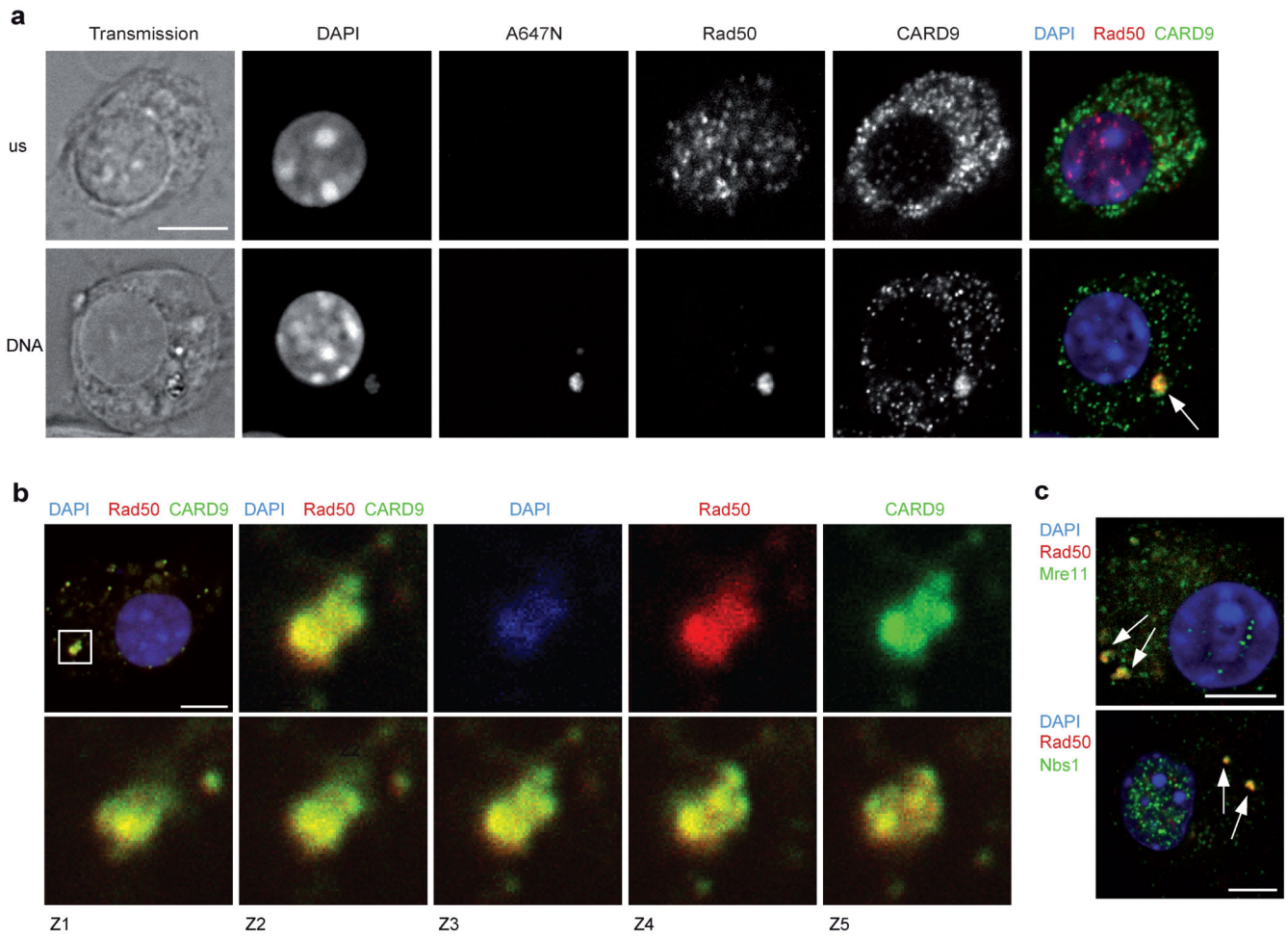

Figure 2. CARD9 is recruited to cytoplasmic dsDNA-sensing Rad50 complexes

(**a-c**) Confocal microscopy analysis. (**a**) BMDCs were left unstimulated (us) or were transfected with ATTO 647N (A647N) fluorescently labeled poly(dG:dC) (DNA) (2.5 μg/ml) for 2 hours and then stained with DAPI as a DNA counterstain and antibodies against Rad50 and CARD9. The arrow in the merged picture indicates a representative cytosolic dsDNA/Rad50/CARD9 complex. (**b**) BMDCs were transfected with dsDNA, stained, and analyzed as in (**a**). A dsDNA/Rad50/CARD9 complex (upper left picture, box) was visualized at higher magnifications and in different z-layers (z1 – z5). (**c**) BMDCs were transfected with dsDNA as in (**a**) and stained with DAPI and antibodies against Rad50 and Mre11 or Nbs1. Cytosolic dsDNA/Rad50/Mre11 or dsDNA/Rad50/Nbs1 complexes are indicated by arrows. Scale bars represent 5 μm, and the data are representative of at least three independent experiments in which at least 50 individual cells were analyzed per experiment and assay point.

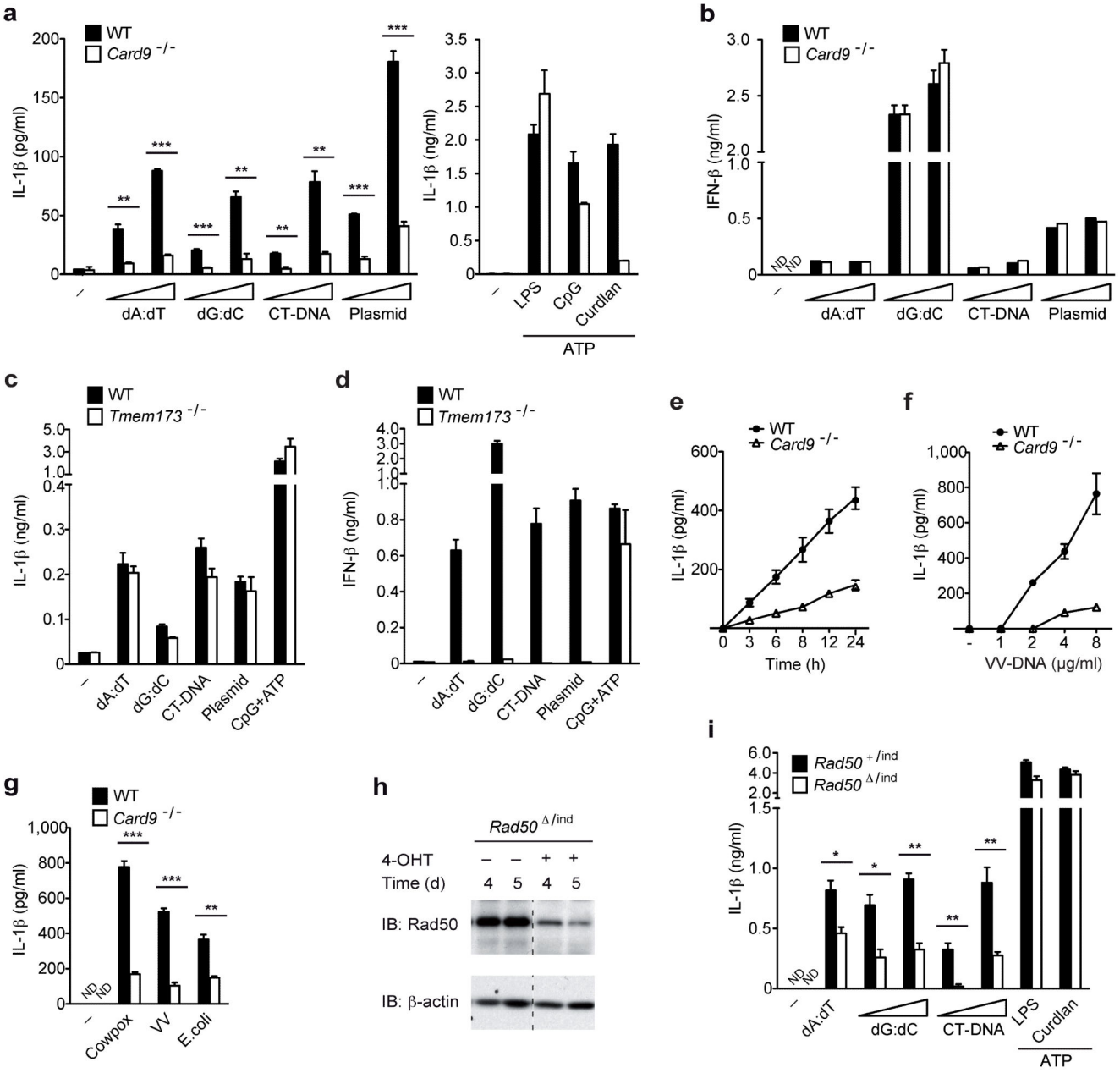

Figure 3. CARD9 and Rad50 are essential for DNA-induced IL-1β production

(**a, b**) BMDCs from WT and *Card9*$^{-/-}$ mice were transfected with dsDNA (1 - 4 μg/ml) of different origins, or stimulated with LPS, CpG, and curdlan plus ATP for 6 hours. IL-1β (**a**) and IFN-β (**b**) concentrations in the supernatants were determined. (**c, d**) BMDCs from WT and *Tmem173*$^{-/-}$ mice were transfected with dsDNA or stimulated with CpG + ATP as in (**a, b**). IL-1β (**c**) and IFN-β (**d**) concentrations were determined in the supernatants. (**e**) BMDCs were transfected with poly(dG:dC) (4 μg/ml) for the indicated time period. (**f**) BMDCs were transfected with increasing amounts of purified dsDNA from vaccinia virus (VV-DNA) for 16 hours. (**g**) BMDCs were transfected with the indicated microbial DNA for 16 hours, and the IL-1β levels in the supernatants were determined. (**h, i**) Dendritic cells were

differentiated from murine bone marrow of the indicated genotype; 4-hydroxy-tamoxifen (4-OHT) was added on culture day 5. (**h**) BMDCs (with or without 4-OHT treatment) were lysed at the indicated time after the addition of 4-OHT. The Rad50 and β-actin protein levels in the cellular lysates were analyzed by western blotting. (**i**) At 5 days after the addition of 4-OHT, BMDCs were transfected with dsDNA (1 - 4 μg/ml) or stimulated with LPS + ATP and curdlan + ATP, and IL-1β concentrations in the supernatants were determined. The data are represented as the mean + SEM of triplicates. One representative of at least three independent experiments is shown. *$p < 0.05$, **$p < 0.01$, ***$p < 0.01$, Student's t-test. ND, not detectable.

Europe PMC Funders Author Manuscripts

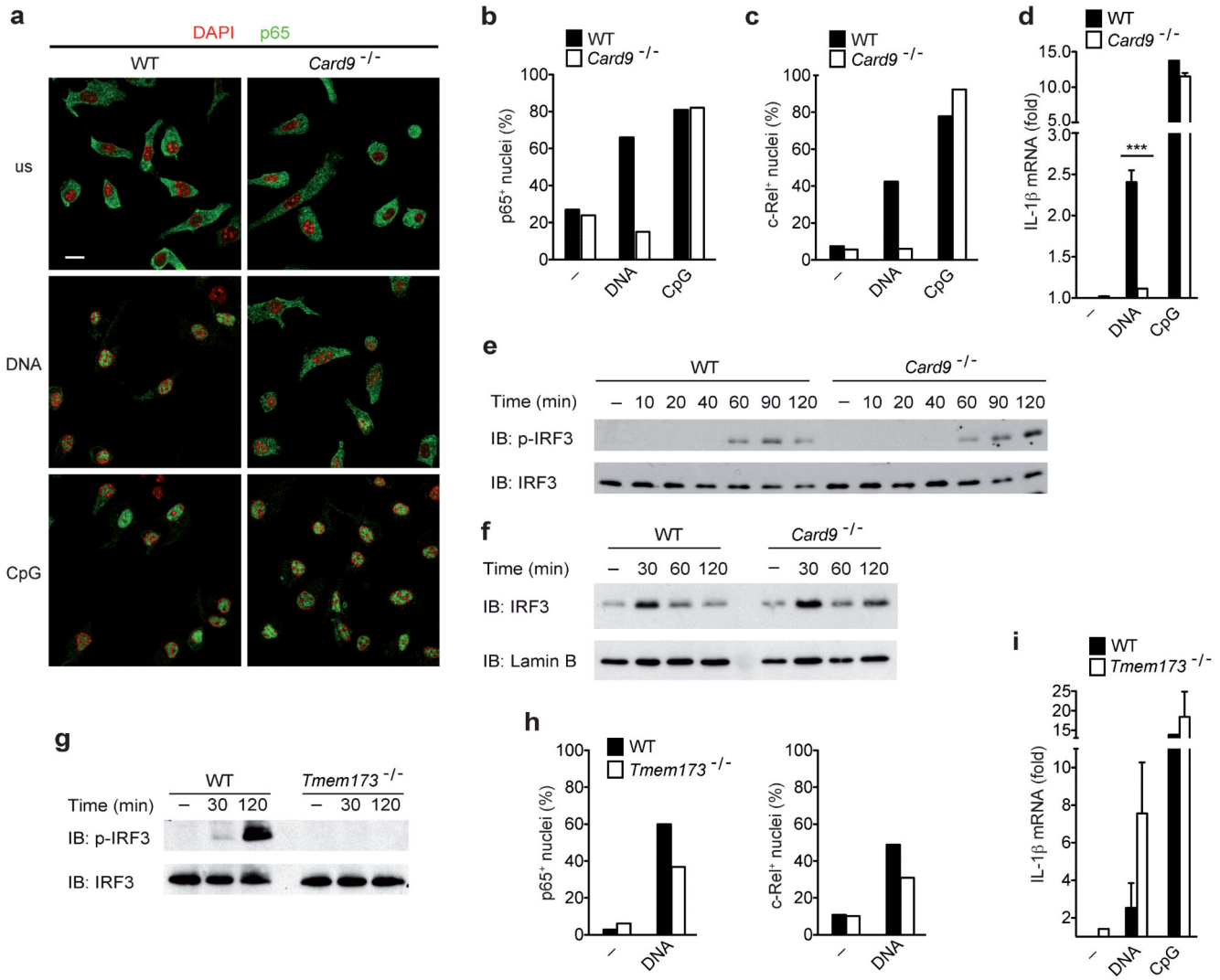

Figure 4. CARD9 controls dsDNA-mediated NF-κB activity

(**a-c**) BMDCs from WT or *Card9*$^{-/-}$ mice were left untreated (us), transfected with poly(dG:dC) (DNA) (2.5 μg/ml), or stimulated with CpG for 1 hour, and subsequently fixed and stained with DAPI and an anti-p65 or anti-c-Rel antibody. p65 and c-Rel translocation into the nucleus was monitored by confocal microscopy and quantified by determining the frequency of p65- or c-Rel-positive nuclei in at least 100 individual cells. The scale bar represents 5 μm. (**d**) BMDCs were left untreated, transfected with poly(dG:dC) (DNA) (2.5 μg/ml), or stimulated with CpG for 4 hours, and IL-1β transcript levels were measured by quantitative real-time PCR and normalized to β-actin mRNA levels. The data are shown as the mean + SEM. ***$p < 0.001$, Student's t-test. (**e, f**) WT or *Card9*$^{-/-}$ BMDCs were transfected with dsDNA for the indicated time. (**e**) Immunoblot analysis of cytosolic extracts. The blots were probed with an antibody against phospho-IRF3 (Ser396) or IRF3. (**f**) Nuclear extracts were immunoblotted with anti-IRF3 and anti-Lamin B antibodies. (**g**) BMDCs from WT and *Tmem173*$^{-/-}$ mice were stimulated and analysed as in (**e**). (**h**) WT or *Tmem173*$^{-/-}$ BMDCs were left untreated or transfected with dsDNA, and analysed as in (**a-**

c). (**i**) BMDCs from WT and *Tmem173*$^{-/-}$ mice were treated and analysed as in (**d**).The data are representative of two (**i**) or three (**a-h**) independent experiments.

Europe PMC Funders Author Manuscripts

Europe PMC Funders Author Manuscripts

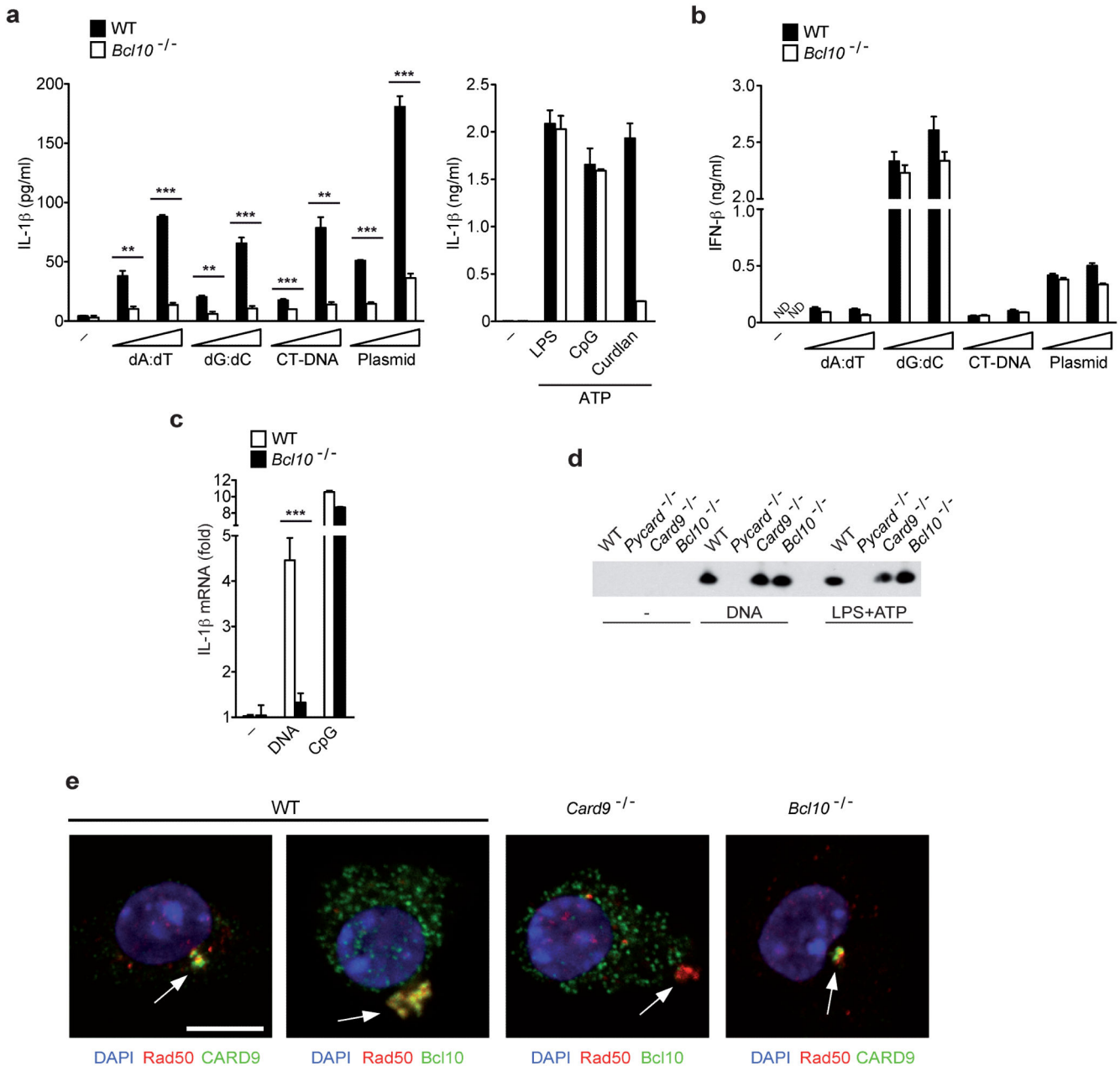

Figure 5. Rad50/CARD9 interactions recruit Bcl10 for IL-1β responses

IL-1β (**a**) and IFN-β (**b**) concentrations were measured in the supernatants of BMDCs transfected with dsDNA (1 - 4 μg/ml) of different origins. LPS, CpG, and curdlan plus ATP were used as controls. The data are shown as the mean + SEM. (**c**) BMDCs were left untreated or transfected with poly(dG:dC) (DNA) (2.5 μg/ml) or stimulated with CpG for 4 hours. IL-1β transcript levels were measured by quantitative real-time PCR and normalized to β-actin mRNA levels. The data are shown as the mean + SEM. (**d**) BMDCs of the indicated genotypes were transfected with poly(dG:dC) (DNA), or stimulated with LPS +ATP for 8 hours. Caspase-1 p10 protein levels in the tissue culture supernatants were analysed by immunoblot. (**e**) BMDCs of the indicated genotypes were transfected with

poly(dG:dC) (DNA) for 2 hours and analyzed by confocal microscopy following immunofluorescence staining with antibodies against Rad50 and CARD9 or Bcl10; DNA was stained with DAPI. The merged images are shown; the arrows indicate cytosolic dsDNA/Rad50/CARD9, dsDNA/Rad50/Bcl10, or dsDNA/Rad50 complexes. The scale bar represents 5 μm. At least 50 individual cells were analyzed per experiment and assay point. All data are representative of at least three independent experiments. ***$p < 0.001$, Student's t-test. ND, not detectable.

Europe PMC Funders Author Manuscripts

Europe PMC Funders Author Manuscripts

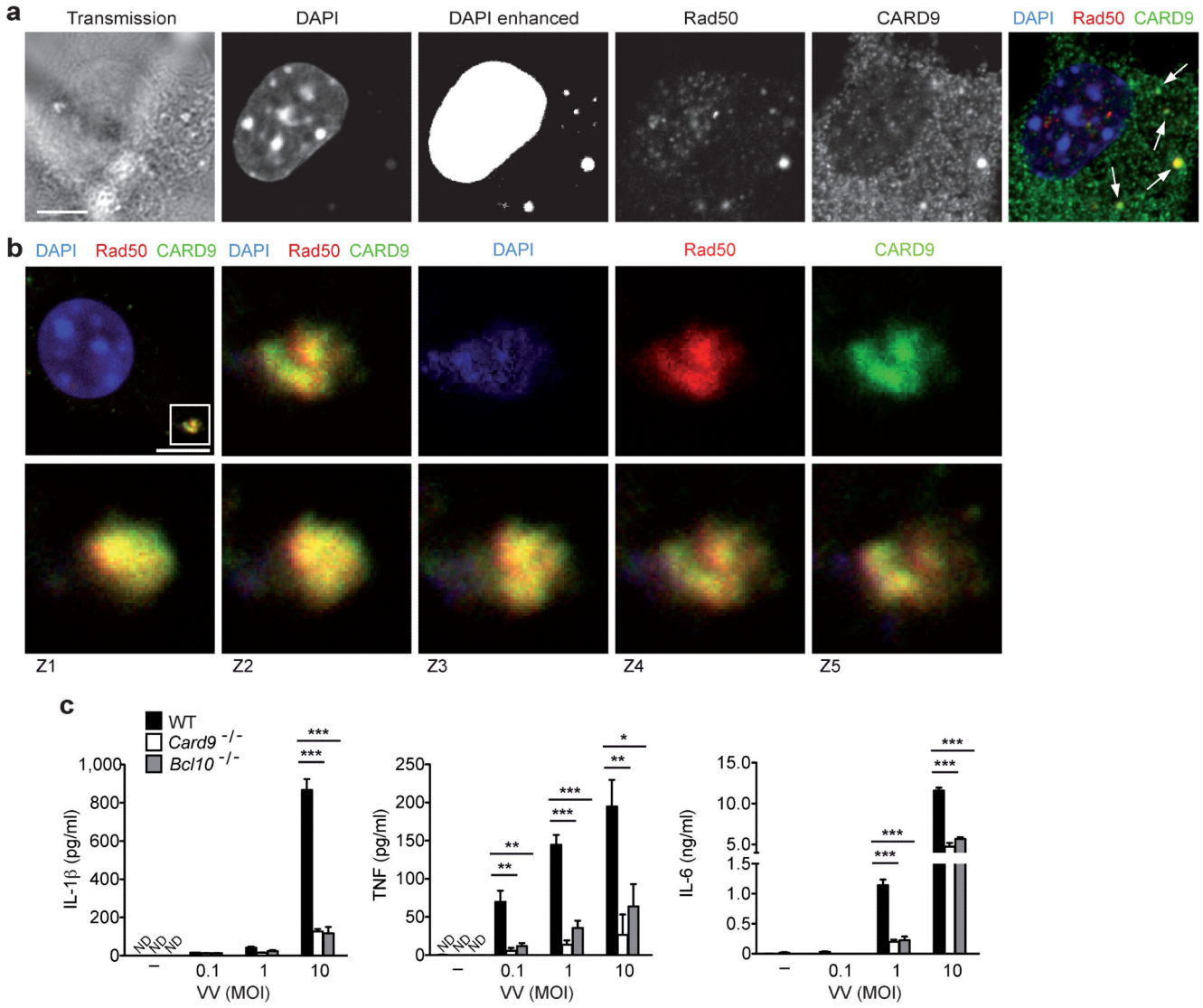

Figure 6. Recognition of DNA virus infection by Rad50/CARD9 complexes

(**a, b**) BMDCs were infected with VV, fixed, and stained with antibodies against Rad50 and CARD9. The cells were analyzed using confocal microscopy; dsDNA was stained with DAPI. The arrows indicate viral-dsDNA/Rad50/CARD9 complexes (**a**). In (**b**), the indicated viral-dsDNA/Rad50/CARD9 complex (upper left picture, box) was visualized at higher magnifications and in different z-layers (z1 - z5). Scale bars, 5 μm. One representative of three independent experiments is shown. (**c**) BMDCs of the indicated genotype were infected with increasing MOIs of VV, and IL-1β, TNF, and IL-6 concentrations were measured in the supernatants. The data are represented as the mean + SEM. *p < 0.05, **p < 0.01, ***p < 0.001, Student's t-test.

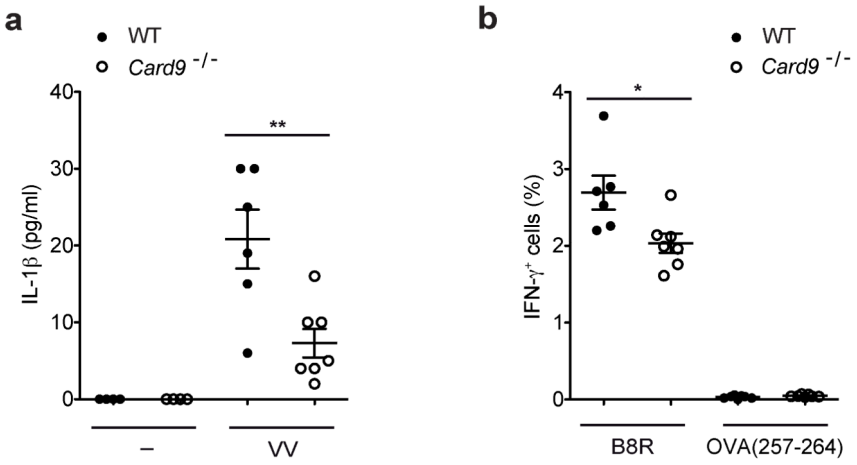

Figure 7. CARD9 controls DNA virus-induced immune responses *in vivo*

(**a**) WT and *Card9*$^{-/-}$ mice were infected with VV *in vivo*, and the IL-1β concentrations were measured in the serum after 6 hours. (**b**) At 8 days post-infection, splenocytes were isolated and stimulated with a VV-specific peptide (B8R) or a control peptide, OVA(257-264), for 5 hours. The percentage of IFN-γ^{+} CD8^{+} T cells was determined by flow cytometry. Circles represent individual mice. The data represent the mean +/− SEM. *p < 0.05, **p < 0.01, Student's t-test.

Europe PMC Funders Author Manuscripts